12^{th} International Conference on Fracture Mechanics of Concrete and Concrete Structures
FraMCoS-12
B.L.A. Pichler, Ch. Hellmich, P. Preinstorfer (Eds)

https://doi.org/10.21012/FC12.1294
MS13-3:1

EARLY-AGE STRENGTH DEVELOPMENT OF CEMENT PASTES MADE OF CEM I, LIMESTONE, AND CALCINED CLAY: THE GOVERNING ROLE OF OPC HYDRATION

SOPHIE J. SCHMID[*,†], **MARKUS KÖNIGSBERGER**[*], **AND BERNHARD PICHLER**[*]

[*] Technische Universität Wien, Institute of Mechanics of Materials and Structures
Karlsplatz 13, 1040 Vienna, Austria
https://www.tuwien.at/cee/imws

[†]Correspondence to Sophie J. Schmid: sophie.schmid@tuwien.ac.at

Key words: Multiscale Strength Modeling, Limestone calcined clay cement paste, OPC hydration

Abstract. The study quantitatively investigates to which extent the hydration of ordinary Portland cement (OPC) contributes to the early-age strength evolution of cement pastes produced with binders containing OPC and limestone (acronym LPC) as well as OPC, limestone, and calcined clay (acronym LC3), respectively. A multiscale strength model for OPC pastes is adapted to binary and ternary mixtures made of CEM I, limestone, and calcined clay. To this end, limestone and calcined clay are introduced as chemically inert spherical inclusion phases which are embedded (next to reactive cement clinker grains) in the hydrate foam matrix. The volume fractions are calculated using Powers' hydration model extended towards consideration of the two additional inert inclusion phases. Elastic phase properties are taken from the literature. The strength predictions for the OPC, LPC, and LC3 pastes are checked against strength values obtained from compressive strength testing during the first week after paste production. The study shows that the OPC hydration plays a governing role when it comes to the early-age strength development of the LPC and LC3 pastes.

1 INTRODUCTION

Compressive strength testing is the most important technique for the assessment of the mechanical performance of cementitious materials. Strength tests are destructive experiments and require several steps of preparation. The raw materials are mixed to become a homogeneous cement paste. The produced material is cast into macroscopic molds. This is followed by curing until the specimen reaches the material age at which strength tests are to be performed. Finally, the specimens are crushed. These steps require manual work and technical equipment such as casting aids and a testing machine. Comprehensive studies involving several different raw materials and and several different initial water-to-binder mass ratios quickly become a a time- and resource-intensive endeavor. This is specifically true for blended cements containing CEM I and up to several types of supplementary cementitious materials (SCMs), because of the large number of design variables, including the OPC replacement ratio, the SCM dosages, the initial water-to-binder mass ratio, the curing temperature, and the material age at testing. Blended cements, such as e.g. limestone Portland cement (LPC) [1] or limestone calcined clay cement (LC3) [2], have a reduced clinker content and, therefore, a smaller environmental footprint [3]. The strength development of the cement pastes depends on the mix design, the properties of the raw materials used,

and the curing conditions.

Material modeling complements experimental efforts. For OPC pastes, a multiscale strength model was developed [4]. It accounts for the hydration-induced evolution of the microstructural phase assemblage in a qualitative and quantitative fashion. In the case of blended binary or ternary cements containing reactive SCMs, generally valid and simple-to-implement models for the evolution of the phase assemblage are, so far, not available. Thus, advanced material characterization is necessary to experimentally determine the phase assemblage evolution which is required as input for a multiscale model model.

This study quantitatively investigates the extent to which an extended OPC model can be used to predict the uniaxial compressive strength of an LPC and an LC3 paste. The validated OPC strength model [4–6] is extended towards the consideration of inert spherical inclusion phases. The modeled strength values are checked against results from uniaxial compressive strength tests, which have been carried out during the first week after material production [7].

The contribution is organized as follows: Section 2 provides equations describing the evolution of phase volume fractions of the extended multiscale strength model. It is applied to selected materials in Section 3. This is followed by the comparison of modeled and experimental strength values and the discussion of results in Section 4. Conclusions drawn from the study are presented in Section 5.

2 PHASE EVOLUTION EQUATIONS FOR THE EXTENDED MULTISCALE STRENGTH MODEL FOR OPC/LPC/LC3 PASTES AT EARLY MATERIAL AGES

The validated multiscale strength model for OPC pastes [4–6] is extended to account for the partial replacement of CEM I with up to two types of supplementary cementitious materials (SCMs). The input and key equations of the multiscale strength model are provided in the following subsections. The focus of the actual study is on ordinary Portland cement (OPC) pastes, limestone Portland cement (LPC) pastes, and limestone calcined clay cement (LC3) pastes.

2.1 Input for the extended multiscale model

Multiscale modeling requires qualitative and quantitative input. Qualitative input refers to the hierarchical organization, characteristic phase shapes, and phase interaction. Quantitative input refers to phase volume fractions and the mechanical properties of the material phases, i.e. of the quasi-homogeneous constituents of cement paste.

Material organograms are two-dimensional sketches illustrating three-dimensional representative volume elements (RVE) and thus, the hierarchical organization, the phase shapes, and the type of phase interaction. Cement paste is treated as a two-scale material [4]. The smaller RVE refers to the scale of the hydrate foam. It consists of a highly disordered arrangement of hydrate gel needles which are randomly oriented in space and which directly interact with water- or air-filled spherical capillary pores. The characteristic size of the hydrate foam-related RVE amounts to some $20\ \mu\mathrm{m}$ [4]. The polycrystalline phase interaction is considered by using the self-consistent homogenization scheme for modeling [8–10]. The larger RVE refers to the scale of the cement paste. It is a matrix-inclusion composite, consisting of spherical CEM I particles and inert inclusions such as limestone and calcined clay, which are embedded in the hydrate foam matrix. The characteristic size of the cement paste-related RVE amounts to some $0.7\,\mathrm{mm}$ [4]. The matrix-inclusion-type phase interaction is considered by using the Mori-Tanaka homogenization scheme for modeling [11, 12].

The cement paste-related volume fractions are computed based on Powers' hydration model [13]. Herein, the related formulae are modified to account for additional inert SCM inclusion phases. This is accomplished by multiplying the original equations by the factor

$[1 - f_{SCM}^{cp}]$, where the cement paste-related volume fraction of the inert material constituents amounts to $f_{SCM}^{cp} = f_{ls}^{cp} + f_{cc}^{cp}$, with

$$f_{ls}^{cp} = \frac{\frac{\rho_{cem}}{\rho_{ls}} \frac{m_{ls}}{m_{cem}}}{\sum_{i=1}^{4} \frac{\rho_{cem}}{\rho_i} \frac{m_i}{m_{cem}}}, \tag{1}$$

$$f_{cc}^{cp} = \frac{\frac{\rho_{cem}}{\rho_{cc}} \frac{m_{cc}}{m_{cem}}}{\sum_{i=1}^{4} \frac{\rho_{cem}}{\rho_i} \frac{m_i}{m_{cem}}}. \tag{2}$$

Thereby, f_{ls}^{cp} and f_{cc}^{cp} stand for the cement paste-related volume fractions of limestone and calcined clay. ρ_i and m_i denote the mass density and initial mass of a specific constituent i, where $i \in \{1{=}cem, 2{=}ls, 3{=}cc, 4{=}wat\}$ refer to the cement paste constituents "cement", "limestone", "calcined clay", and "water", respectively. The modified Powers' equations read as:

$$f_{cem}^{cp} = \frac{1 - \xi}{1 + \frac{\rho_{cem}}{\rho_{wat}} \frac{m_{wat}}{m_{cem}}} \left[1 - f_{SCM}^{cp}\right], \tag{3}$$

$$f_{wat}^{cp} = \frac{\frac{\rho_{cem}}{\rho_{wat}} \left[\frac{m_{wat}}{m_{cem}} - 0.42\,\xi\right]}{1 + \frac{\rho_{cem}}{\rho_{wat}} \frac{m_{wat}}{m_{cem}}} \left[1 - f_{SCM}^{cp}\right], \tag{4}$$

$$f_{hyd}^{cp} = \frac{1.42\,\frac{\rho_{cem}}{\rho_{hyd}}\,\xi}{1 + \frac{\rho_{cem}}{\rho_{wat}} \frac{m_{wat}}{m_{cem}}} \left[1 - f_{SCM}^{cp}\right], \tag{5}$$

$$f_{air}^{cp} = 1 - \left(f_{cem}^{cp} + f_{wat}^{cp} + f_{hyd}^{cp} + f_{SCM}^{cp}\right), \tag{6}$$

where ξ denotes the hydration degree, ρ_{hyd} the mass density of the hydrates, and f_p^{cp} with $p \in \{cem, wat, hyd, air\}$ the cement paste-related volume fractions of "cement", "water", "hydrates", and "air". The sum of all cement paste-related volume fractions, see Eqs. (1)–(6), is equal to 1. The cement paste-related volume fraction of the hydrate foam follows as:

$$f_{hf}^{cp} = 1 - \left(f_{cem}^{cp} + f_{SCM}^{cp}\right). \tag{7}$$

The hydrate foam-related volume fractions of the hydrate gel needles and capillary pores result from the cement paste-related volume fractions of water, hydrates, and air as $f_p^{hf} = f_p^{cp} / f_{hf}^{cp}$, with $p \in \{wat, hyd, air\}$ and $f_{por}^{hf} = f_{wat}^{hf} + f_{air}^{hf}$. This yields

$$f_{hyd}^{hf} = \frac{1.42\,\frac{\rho_{cem}}{\rho_{wat}}\,\xi}{\frac{\rho_{hyd}}{\rho_{wat}}\left[\frac{\rho_{cem}}{\rho_{wat}} \frac{m_{wat}}{m_{cem}} + \xi\right]}, \tag{8}$$

$$f_{por}^{hf} = 1 - f_{hyd}^{hf}. \tag{9}$$

The sum of the two hydrate foam-related volume fractions, see Eqs. (8)–(9), is equal to 1.

The elastic constants of the cement paste constituents are provided in terms of the bulk modulus k_p and the shear modulus μ_p. Numerical values are taken from the literature, see Table 1. Since drained conditions are considered, the bulk modulus and shear modulus of water are zero [14].

Table 1: Bulk modulus k_p and shear modulus μ_p of the p OPC/LPC/LC3 paste constituents, where $p \in \{cem, ls, cc, hyd\}$.

phase	p	k_p [GPa]	μ_p [GPa]	source
CEM I	cem	116.58	53.81	[15]
limestone	ls	73.30	32.00	[16]
calcined clay	cc	47.90	19.70	[17]
hydrates	hyd	18.69	11.76	[4]

2.2 Upscaling the strength of the hydrate gel needles to the macroscopic strength of cement paste; after [6]

A macroscopic uniaxial compressive stress state $\boldsymbol{\Sigma}_{cp}$ acting in $\underline{e}_3$-direction on a cement paste RVE is downscaled to the weakest components of the microstructure, the microscopic hydrate gel needles. This allows for determining whether or not $\boldsymbol{\Sigma}_{cp}$ induces failure in the cement paste. The quasi-brittle, pressure-sensitive shear failure of hydrate gel needles is modeled by means of a Drucker-Prager criterion, $\mathcal{F}_{\text{DP}}$, with the Drucker-Prager constants $k_{hyd}^{\text{DP}} = 60.68\,\text{MPa}$ and $\alpha_{hyd}^{\text{DP}} = 0.258$ [6]. It allows for assessing the integrity ($\mathcal{F}_{\text{DP}} < 0$) or failure ($\mathcal{F}_{\text{DP}} = 0$) of hydrate gel needles based on energy-density-based "higher-order" stress averages. The latter also account for the spatial orientation of the hydrate gel needles.

The scalar volumetric and deviatoric stress values entering the failure criterion are a function of the macroscopic stress state imposed on the RVE, the homogenized elastic stiffness of the cement paste, as well as the properties of the hydrate gel needles, i.e. their volume fraction, their bulk modulus, and their shear modulus [4]. The ultimate compressive stress sustained by the cement paste is determined in two steps: (i) identifying the direction of the most heavily loaded hydrate gel needles and (ii) increasing the macroscopic uniaxial compressive stress to failure ($\mathcal{F}_{\text{DP}} = 0$), resulting in the ultimate compressive stress sustained by the material, see [4–6, 14] for more details.

3 STRENGTH MODEL APPLICATION

3.1 Materials

The extended strength model is applied to the three cement pastes analyzed in [7]. They are made of three binders. The OPC binder contains only CEM I-52.5 R. The LPC binder is a mixture of $70\,\%$ by mass of the same CEM I and $30\,\%$ by mass limestone. The LC3 binder contains $70\,\%$ by mass of the same CEM I, $15\,\%$ by mass limestone, and $15\,\%$ by mass calcined clay. The cement pastes are produced with a water-to-binder mass ratio of $w/b = 0.45$. The effective water-to-OPC mass ratio is obtained from the cement paste recipes:

$$\frac{m_{wat}}{m_{cem}} = w/b \left[1 + \frac{m_{ls}}{m_{cem}} + \frac{m_{cc}}{m_{cem}}\right] . \quad (10)$$

Strength test results and the cumulative heat release obtained from isothermal calorimetry testing can be found in [7].

3.2 Material-specific input

The determination of the volume fractions according to Eqs. (1)–(9) require binder-specific properties such as the mass density and the initial cement paste composition, see Tables 2 and 3. Elastic constants are taken from Table 1.

Table 2: Mass densities of the cement paste constituents.

	mass density	**source**
CEM I	$3.13\,\mathrm{g/cm^2}$	data sheet
limestone	$2.70\,\mathrm{g/cm^2}$	[18]
calcined clay	$2.60\,\mathrm{g/cm^2}$	data sheet
water	$1.00\,\mathrm{g/cm^2}$	-
hydrates	$2.07\,\mathrm{g/cm^2}$	[19]

Table 3: Initial limestone/calcined clay/water-to-OPC mass ratios for the OPC, LPC, and LC3 pastes.

	OPC	LPC	LC3
m_{ls}/m_{cem}	0.000	0.429	0.214
m_{cc}/m_{cem}	0.000	0.000	0.214
m_{wat}/m_{cem}	0.450	0.643	0.643

3.3 Material-specific strength prediction

The extended multiscale strength model is used to predict the early-age strength evolution of the three cement pastes. Thus, the micromechanical model is evaluated for two m_{wat}/m_{cem} values, i.e. for 0.45 being representative for the OPC paste and for 0.64 being representative for the LPC and LC3 pastes, respectively. The qualitative input is taken from Subsection 2.1. The quantitative input is taken from Tables 1–3, and Eqs. (1)–(9). The compressive strength of cement paste is predicted for hydration degrees ranging between 0 and 1, see Fig. 1.

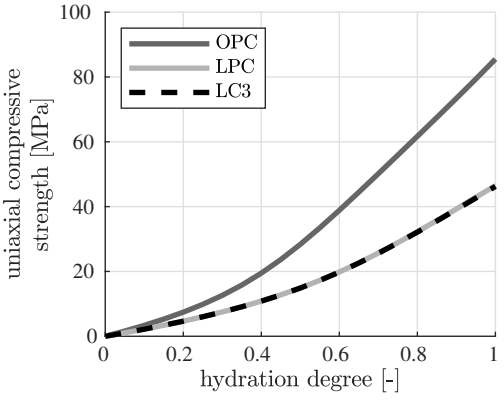

Figure 1: Model-predicted uniaxial compressive strength of the OPC, LPC, and LC3 pastes, as a function of the hydration degree.

The model-predicted strength values of the LPC and LC3 pastes are virtually identical, as both cement pastes have the same value of m_{wat}/m_{cem}. Small deviations are only due to the different stiffness and mass densities of limestone and calcined clay.

4 DISCUSSION

4.1 Comparison of model-predicted and experimental data

Model predictions of the uniaxial compressive strength of the cement pastes are illustrated as a function of the hydration degree, see Fig. 1. The uniaxial compressive strength is characterized as a function of the material age [7]. Thus, the comparison of the modeled and experimental strength values needs further discussion.

For OPC pastes, the hydration degree is proportional to the specific cumulative heat release [20]:

$$\xi(t) = \frac{Q(t)}{\ell_h}\,, \tag{11}$$

where t is the time variable and ℓ_h denotes the latent heat of CEM I. Thus, the multiplication of the hydration degree by the latent heat of CEM I, allows for representing the model-predicted uniaxial compressive strength as a function of the specific cumulative heat release, see the solid curves in Fig. 2. The latent heat is prescribed with $\ell_h = 500\,\mathrm{J/g}$ [20]. This approach is also applicable for the LPC and LC3 pastes, because limestone and calcined clay are assumed to be inert material phases. The total heat release is therefore related to the CEM I hydration only, similar to the OPC paste.

The experimentally obtained uniaxial compressive strength values are also plotted over the cumulative heat release per gram of CEM I in the initial binder composition, see the symbols in Fig. 2. This is possible by reading the cumulative heat release values, from isothermal calorimetry testing results, at the same time instants at which strength testing was carried out, and by referring the strength test data to these cumulative heat release values.

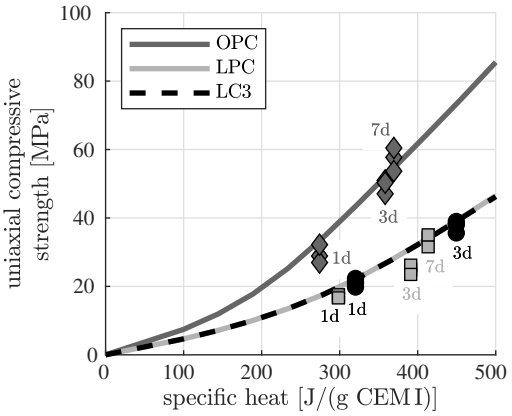

Figure 2: Model-predicted (solid lines) and experimental (symbols) uniaxial compressive strength of the OPC, LPC, and LC3 pastes, as a function of the specific cumulative heat release per gram CEM I, being available in the initial binder composition: the hydration degree from Fig. 1 is scaled by the latent heat of $500\,\mathrm{J/g}$, and time instants of strength testing are converted to the specific cumulative heat release using data from isothermal calorimetry.

The model-predicted strength values agree well with the experimental strength values. Thus, the extended multiscale strength model provides a good estimation of early-age strength development also for binary and ternary blended cement pastes, at least for the here investigated materials. This indicates that the hydration of CEM I plays a governing role for the early-age strength development of limestone- and calcined clay-blended cement pastes.

4.2 Limitations of the study and future outlook

The present study includes the following limitations. Limestone and calcined clay are considered as inert material phases. Modeled and experimental strength values are compared for only three types of cement pastes which are composed of one type of cement, limestone, and calcined clay, respectively. For this, the latent heat of the pastes was prescribed at $500\,\mathrm{J/g}$. Future research should expand the range of materials analyzed by including additional OPC, LPC, and LC3 pastes, preferable made from different raw materials and different initial water-to-binder mass ratios [21].

5 SUMMARY AND CONCLUSIONS

A validated multiscale strength model for ordinary Portland cement (OPC) pastes was extended towards the consideration of limestone and calcined clay as inert material phases. The model uses a hierarchical, two-scale material representation for cement pastes. The cement paste and hydrate foam-related volume fractions were determined based on modified Powers' hydration model with the OPC-related hydration degree as the maturity parameter. A Drucker-Prager failure criterion was used to model the microscopic pressure-sensitive shear failure of the hydrate gel needles under compressive loading, in combination with energy-density-based stress averages providing the link between macroscopic loading of cement paste and microscopic stresses experienced by hydrate gel needles with specific spatial orientation. The model was applied to cement pastes which were experimentally characterized in [7]. The investigated LPC and LC3 pastes have similar strength evolutions, when plotted as a function of the OPC-related hydration degree, due to their comparable initial water-to-OPC mass ratios. In order to compare model predictions of the compressive strength with experimental data, both types of strength were plotted as a function of the cumulative heat release. The model-predicted strength values agree well with the experimentally determined strength values. Deviations are particularly observed for the LPC paste one and three days after paste production. The study reveals that the extended multiscale strength model allows for a good estimation of the early-age uniaxial compressive strength also for blended cements, at least for the here-investigated materials, and that the OPC hydration plays a governing role when it comes to the strength evolution at early material ages.

ACKNOWLEDGMENT

The authors would like to thank Dr. Alexandre Ouzia (Heidelberg Materials) for fruitful discussions. The first author gratefully acknowledges financial support through the MatCHMaker project which has received funding from the European Union's Horizon Europe research and innovation programme under grant agreement N° 101091687.

REFERENCES

[1] B. Lothenbach, G. Le Saout, E. Gallucci, and K. Scrivener. Influence of limestone on the hydration of Portland cements. *Cement and Concrete Research*, 38(6):848–860, 2008.

[2] M. Antoni, J. Rossen, F. Martirena, and K. Scrivener. Cement substitution by a combination of metakaolin and limestone. *Cement and Concrete Research*, 42(12):1579–1589, 2012.

[3] K. Scrivener, F. Martirena, S. Bishnoi, and S. Maity. Calcined clay limestone cements (LC3). *Cement and Concrete Research*, 114:49–56, 2018.

[4] B. Pichler and C. Hellmich. Upscaling quasi-brittle strength of cement paste and mortar: A multi-scale engineering mechanics model. *Cement and Concrete Research*, 41(5):467–476, 2011.

[5] B. Pichler, C. Hellmich, J. Eberhardsteiner, J. Wasserbauer, P. Termkhajornkit, R. Barbarulo, and G. Chanvillard. Effect of gel-space ratio and microstructure on strength of hydrating cementitious materials: An engineering micromechanics approach. *Cement and Concrete Research*, 45:55–68, 2013.

[6] M. Königsberger, M. Hlobil, B. Delsaute, S. Staquet, C. Hellmich, and B. Pichler. Hydrate failure in ITZ governs concrete strength: A micro-to-macro validated engineering mechanics model. *Cement and Concrete Research*, 103:77–94, 2018.

[7] S.J. Schmid, L. Zelaya, O. Lahayne, M. Peyerl, and B. Pichler. Hourly three-minute creep testing of an LC3 paste at early ages: Advanced test evaluation and

the effects of the pozzolanic reaction on shrinkage, elastic stiffness, and creep. *Cement and Concrete Research*, 187:107705, 2025.

[8] A.V. Hershey. The elasticity of an isotropic aggregate of anisotropic cubic crystals. *Journal of Applied Mechanics*, 21(3):236–240, 1954.

[9] E. Kröner. Berechnung der elastischen Konstanten des Vielkristalls aus den Konstanten des Einkristalls. *Zeitschrift für Physik A Hadrons and Nuclei*, 151(4):504–518, 1958.

[10] R. Hill. A self-consistent mechanics of composite materials. *Journal of the Mechanics and Physics of Solids*, 13(4):213–222, 1965.

[11] T. Mori and K. Tanaka. Average stress in matrix and average elastic energy of materials with misfitting inclusions. *Acta metallurgica*, 21(5):571–574, 1973.

[12] Y. Benveniste. A new approach to the application of Mori-Tanaka's theory in composite materials. *Mechanics of materials*, 6(2):147–157, 1987.

[13] T.C. Powers and T.L. Brownyard. Studies of the physical properties of hardened portland cement paste. In *Journal Proceedings*, pages 549–602, 1947.

[14] B. Pichler, C. Hellmich, and J. Eberhardsteiner. Spherical and acicular representation of hydrates in a micromechanical model for cement paste: prediction of early-age elasticity and strength. *Acta Mechanica*, 203(3):137–162, 2009.

[15] K. Velez, S. Maximilien, D. Damidot, G. Fantozzi, and F. Sorrentino. Determination by nanoindentation of elastic modulus and hardness of pure constituents of Portland cement clinker. *Cement and Concrete Research*, 31(4):555–561, 2001.

[16] R.F.S. Hearmon. The elastic constants of crystals and other anisotropic materials. *Landolt-Börnstein Tables*, 3(18):559, 1984.

[17] Z. Wang, H. Wang, and M.E. Cates. Effective elastic properties of solid clays. *Geophysics*, 66(2):428–440, 2001.

[18] J.D. Bass et al. Elasticity of minerals, glasses, and melts. *Mineral physics and crystallography: A handbook of physical constants*, 2:45–63, 1995.

[19] G. Constantinides and F.-J. Ulm. The effect of two types of CSH on the elasticity of cement-based materials: Results from nanoindentation and micromechanical modeling. *Cement and Concrete Research*, 34(1):67–80, 2004.

[20] J. Byfors. *Plain concrete at early ages*. Swedish Cement and Concrete Research Institute, 1980. Stockholm, Sweden.

[21] S.J. Schmid et al. Porosity gradients, filler effect, and SCM reactivity govern the early-age compressive strength evolution of pure/binary/ternary OPC/limestone/calcined clay cement pastes. *Paper draft under preparation*, 2025.